Rudel, Stefan S.; Deubner, H. Lars; Müller, Matthias; Karttunen, Antti J.; Kraus, Florian

Complexes featuring a linear [N≡U≡N] core isoelectronic to the uranyl cation

Published in:
Nature Chemistry

DOI:
10.1038/s41557-020-0505-5

Published: 01/10/2020

Document Version
Peer-reviewed accepted author manuscript, also known as Final accepted manuscript or Post-print

Please cite the original version:
Rudel, S. S., Deubner, H. L., Müller, M., Karttunen, A. J., & Kraus, F. (2020). Complexes featuring a linear [N≡U≡N] core isoelectronic to the uranyl cation. *Nature Chemistry*, *12*(10), 962-967. https://doi.org/10.1038/s41557-020-0505-5

Complexes featuring a linear [N≡U≡N] core isoelectronic to the uranyl cation

Stefan S. Rudel [1], H. Lars Deubner [1], Matthias Müller [1], Antti J. Karttunen [2], Florian Kraus [1,*]

1 Anorganische Chemie, Fluorchemie, Fachbereich Chemie, Philipps-Universität Marburg, Hans-Meerwein-Str. 4, 35032 Marburg, Germany

2 Department of Chemistry and Materials Science, Aalto University 00076 Aalto, Finland

Abstract

The aqueous chemistry of uranium is dominated by the linear uranyl cation $[UO_2]^{2+}$, yet the isoelectronic nitrogen-based analogue of this ubiquitous cation, molecular $[UN_2]$, has so far only been observed in an argon matrix. Here, we present three different complexes of $[UN_2]$ obtained by the reaction of the uranium pentahalides UCl_5 or UBr_5 with anhydrous liquid ammonia. The $[UN_2]$ moieties are linear, with the U atoms coordinated by five additional ligands (ammonia, chloride or bromide), resulting in a pentagonal bipyramidal coordination sphere that is also commonly adopted by the uranyl cation $[UO_2(L)_5]^{2+}$. In all three cases, the nitrido ligands are further coordinated through their lone pairs by the Lewis acidic ligands $[U(NH_3)_8]^{4+}$ to form almost linear, trinuclear complex cations. Those were characterized by single crystal X-ray diffraction, Raman and IR spectroscopy, $^{14}N/^{15}N$ isotope studies, and quantum chemical calculations which support the presence of U≡N triple bonds within the $[UN_2]$ moieties.

Although the uranyl cation $[UO_2]^{2+}$ is a prevalent species in uranium chemistry, its isoelectronic nitrogen analogue $[UN_2]$ has not been encountered yet outside an argon matrix, as NUN and NUNH species[1–3]. Under these conditions, several complexes of $[UN_2]$ with one to five dinitrogen ligands, $[UN_2(N_2)_x]$ (x = 1 to 5), have also been observed.[4] Beyond the fundamental interest in these species, uranium nitrides are also investigated for their catalytic properties for example for CO_2 or N_2 activation, and as a future fuel in generation IV nuclear reactors as well as in space power and propulsion systems.[5–13]

The investigation of multiple bonding to uranium atoms is also a challenge for experimental and theoretical chemistry alike.[14–16] Previous works used very elaborate ligands to stabilize such compounds in order to counter the high reactivity of terminal uranium nitrides towards organic solvents and reagents.[14,17,18] Here we report on a $[UN_2]$ fragment, a linear $[N{\equiv}U{\equiv}N]$ moiety which is stabilized only by the coordination of two Lewis acidic ammine uranium(IV) cations, ammonia molecules, or halido ligands. These $[UN_2]$-containing species occur as metastable intermediates of the disproportionation and ammonolysis of the uranium pentahalides UCl_5 and UBr_5. Choosing liquid ammonia as both reactant and solvent prevented side reactions leading to non-nitrogen based products from occurring — this circumstance is especially beneficial with regard to the synthesis of ceramic nuclear fuels, where carbide and oxide contamination is detrimental.[10]

Results and Discussion

Synthesis and structural description of the [UN₂] complexes

We reacted UBr_5 with NH_3 at −78 °C and observed the formation of a yellow-green suspension along with a slight evolution of nitrogen gas. The compound $[(NH_3)_8U(\mu\text{-}N)(NH_3)_5U(\mu\text{-}N)U(NH_3)_8]Br_8{\cdot}26NH_3$, (**1**$Br_8{\cdot}26NH_3$), crystallized (idealized Eq. 1) after two weeks at −40 °C. X-ray crystal structure determination under consistent cooling and strict exclusion of air showed a linear tri-nuclear uranium complex with N-bridged uranium atoms (Figure 1a) that are additionally coordinated by NH_3 ligands. The central U atom (U_{cen}) of the $[UN_2]$ unit carries five ammine ligands whereas eight ammine ligands coordinate each of the terminal U atoms (U_{ter}).

$$18\ UBr_5 + 182\ NH_3 \longrightarrow 6\ [U_3(\mu\text{-}N)_2(NH_3)_{21}]^{8+} + 48\ Br^- + 42\ NH_4Br + N_2 \qquad (1)$$

When we reacted UBr_5 with anhydrous ammonia at room temperature in a sealed bomb tube, the chemically related compound $[(NH_3)_8U(\mu\text{-}N)Br(NH_3)_4U(\mu\text{-}N)U(NH_3)_8]_2Br_{14}\cdot 21NH_3$ ($\mathbf{2}Br_7\cdot 10.5NH_3$) was formed (idealized Eq. 2) as evidenced by single-crystal diffraction. In this compound, the central U atom of the $[UN_2]$ unit carries one bromido and four ammine ligands (Figure 1b).

$$18\ UBr_5 + 176\ NH_3 \longrightarrow 6\ \underset{\mathbf{2}}{[U_3Br(\mu\text{-}N)_2(NH_3)_{20}]^{7+}} + 42\ Br^- + 42\ NH_4Br + N_2 \quad (2)$$

A third similar, $[UN_2]$ containing compound, $[(NH_3)_8U(\mu\text{-}N)Cl_2(NH_3)_3U(\mu\text{-}N)U(NH_3)_8]Cl_6\cdot 6NH_3$, ($\mathbf{3}Cl_6\cdot 6NH_3$), crystallized, when we reacted UCl_5 with ammonia at room temperature (idealized Eq. 3).

$$18\ UCl_5 + 170\ NH_3 \longrightarrow 6\ \underset{\mathbf{3}}{[U_3Cl_2(\mu\text{-}N)_2(NH_3)_{19}]^{6+}} + 36\ Cl^- + 42\ NH_4Cl + N_2 \quad (3)$$

Compound $\mathbf{3}Cl_6\cdot 6NH_3$ carries two chloride ligands and three ammine ligands at the U atom of the $[UN_2]$ unit (Figure 1c).

Figure 1 shows the structure of the cations $\mathbf{1}^{8+}$, $\mathbf{2}^{7+}$, and $\mathbf{3}^{6+}$ and some selected U−N distances observed in their crystal structures. The total charge of the cations $\mathbf{1}^{8+}$, $\mathbf{2}^{7+}$, and $\mathbf{3}^{6+}$ is dictated by the number of counter-ions present in the structure. This requires a mixed valence for the three uranium atoms of each complex cation. Regarding the differing lengths of the U_{cen}−(μ-N)−U_{ter} bonds, the only reasonable assignment of oxidation numbers is +VI for the U_{cen} atom, and +IV for the terminally bound U_{ter} atoms. In many nitrogen-bridged uranium complexes, the nitride ligand is stabilized to such an extent that the compounds are better described as imides, U=NR, rather than U≡N.[9,12,19,20] In cation $\mathbf{1}^{8+}$, the U_{cen}−(μ-N) bond lengths of 1.853(3) and 1.854(3) Å are of course longer than those calculated for molecular [N≡U≡N], $[NUN(N_2)_5]$, and $[N{\equiv}UF_3]$ (1.717,[21] 1.753[4] and 1.759 Å,[22] respectively) but close to the terminal U(VI)≡N triple bonds reported for $[U(N)(N(CH_2NSi\textit{i}\text{-}Pr_3)_3)]$ (1.799(7) Å). They are equal, within the tripled standard uncertainty, to those in $[Na(12\text{-}crown\text{-}4)_2][U(N)(N(CH_2NSi\textit{i}\text{-}Pr_3)_3)]$ (1.825(15) Å)[14,18] and considerably shorter than in $(C_6F_5)_3B{-}N{\equiv}U(N[\textit{t}\text{-}Bu](3,5\text{-}Me_2C_6H_3))_3$ (1.880(4) Å).[23] Consequently, the U_{ter}−(μ-N) distances of 2.304(3) and 2.300(3) Å are longer than in single bonded uranium(IV) nitrido complexes like $[(C_5Me_5U(\mu\text{-}I)_2]_3N$ (2.138(3) to 2.157(3) Å).[24] Double bonded imido ligands typically show significantly longer U=N bonds (1.920(2) to 2.086 Å).[25,26] Some uranyl-analogous diimido complexes exhibit extremely short U−N distances in the range of U(VI)≡N triple bonds, like 1.848(4) Å in $[U(N\textit{t}\text{-}Bu)_2I_2(THF)_2]$.[16] This might be attributed to the small coordination number of six and the relatively small ligands. The U_{cen}–(μ-N)–U_{ter} angles of cation $\mathbf{1}^{8+}$ are close to 180° (177.98(14)° and 178.44(17)°), as is the (μ-N)–U_{cen}–(μ-N) angle (179.07(11)°). This is expected for the species [N≡U≡N]. The pentagonal-bipyramidal coordination of the U_{cen} atom is also common in uranyl chemistry.[16,27,28] In light of this we interpret cation $\mathbf{1}^{8+}$ with the Lewis structure depicted in Figure 1a. The central moiety represents the nitrido analogue of a pentaammine uranyl(VI) cation, $[UN_2(NH_3)_5]$, which is stabilized by the weaker coordination of two $[U(NH_3)_8]^{4+}$ cations to the nitrido ligands.

Single crystals of the compound $\mathbf{2}Br_7\cdot10.5NH_3$ revealed the second example of such a cation. Their structure contains two symmetry-independent cations $\mathbf{2}^{7+}$ shown in Figure 1b. In comparison to cation $\mathbf{1}^{8+}$, a bromido ligand lowers the charge of the trinuclear complex to 7+ and displaces one of the five ammine ligands at the central U atom. Compared to the U_{ter} atoms, the U_{cen} atom is the chemically harder since higher valent atom and as such it is preferred by the bromido ligand. The U_{cen}–(μ-N) atom distances of cations $\mathbf{2}^{7+}$ (1.799(8), 1.870(9) Å, and 1.816(9), 1.851(10) Å) are in agreement to those of cations $\mathbf{1}^{8+}$ (and $\mathbf{3}^{6+}$). The two crystallographically independent $[UN_2]$ units are essentially linear with 179.0(4) and 178.6(3)°. The appendant U_{cen}–(μ-N)–U_{ter} angles deviate a little more from linearity with 171.6(5) and 175.4(5)°, and 171.6(5) and 174.1(6)°, which is likely due to the steric demand of the bromido ligand.

$[(NH_3)_8U(\mu\text{-}N)Cl_2(NH_3)_3U(\mu\text{-}N)U(NH_3)_8]Cl_6\cdot6NH_3$, ($\mathbf{3}Cl_6\cdot6NH_3$) is the third example of a $[UN_2]$ complex. Compared to cation $\mathbf{1}^{8+}$, two ammine ligands of the U_{cen} atom are replaced by chlorido ligands (Figure 1c), lowering the total charge of the complex to 6+. Expectedly, the hard Cl^- anion preferably coordinates to the chemically harder U_{cen} atom. For other examples of this coordination behavior see the literature.[27] The U_{cen}–(μ-N) atom distances of $\mathbf{3}^{6+}$ (1.834(5) and 1.853(5) Å) are equal within the doubled standard uncertainty. The appendant U_{cen}–(μ-N)–U_{ter} angles however are with 170.9(3) and 172.4(3)° slightly smaller compared to those in cation $\mathbf{1}^{8+}$, which we attribute to the steric demand of the bound Cl atoms. The U–Cl atom distances (2.837(1) and 2.807(1) Å) in cation $\mathbf{3}^{6+}$ are considerably longer than in $[(py)_3UO_2Cl_2]$ (2.693(1) and 2.734(1) Å),[28] which is attributed to the higher covalence of the U–N bond in comparison to the U–O bond. However, the Cl–U–Cl angle (149.99(4)°) of cation $\mathbf{3}^{6+}$ is still comparable to the corresponding angle of $[(py)_3UO_2Cl_2]$ (146.80(4)°).[28] Supplementary Table 1 holds selected crystallographic data and details of the structure determinations of the title compounds.

For the reaction mechanism, we propose that a dissolved U(V) species disproportionates in ammonia to U(IV) and U(VI) species. It seems like some ammonia is oxidized by such a U(VI) species to N_2, while formation of the trinuclear U complexes that we observe in the solid-state proceeds via deprotonation of ammine ligands. Obviously, the nitrido ligands stabilize the central U(VI) species, while the nitrido complexes become stabilized by the coordination of $[U(NH_3)_8]^{4+}$ complexes.

Crystal-chemical considerations

The very oxophilic nature of uranium could undoubtedly lead to oxygen-containing compounds during the syntheses and the distinction of nitrogen and oxygen atoms in an X-ray experiment is usually regarded as difficult due to the similar atomic form factors. So, one could argue that not $[UN_2]$ but $[UO_2]^{2+}$ or $[UO_2]^{+}$ complexes were obtained instead. Besides our Raman spectroscopic evidence (v.i.) that shows the lack of U−O stretching vibrations but instead a clear isotope shift for a $^{15}NH_3$ enriched compound, and the compliance with our quantum chemical structure optimizations (v.i.), also the crystal structure refinements show differences suitable to distinguish N from O atoms in these cases. A first substantial argument is the number of anions in the unit cell, dictating the total charge of the uranium complexes as **1**$^{8+}$, **2**$^{7+}$, and **3**$^{6+}$. If the μ-bridging atoms were O atoms, all the U atoms would have to be in equal oxidation state (+IV). However, the highly asymmetric position of the bridging atoms between the U_{cen} and the U_{ter} atoms does not correspond to such a model and is additionally in stark contrast with usual U−O bond lengths in other molecular μ-O-bridged uranium complexes, where roughly symmetric bonds with distances around 2.1 Å are encountered.[29–31] However, in our cases we observe atom distances of circa 1.85 Å to the U_{cen} and circa 2.3 Å to the U_{ter} atoms. In consequence, we would have to have overlooked additional anions, or the oxidation states of some U_{ter} atoms would have to be lower if $[UO_2]^{2+}$ or $[UO_2]^{+}$ cations were present. While additional bromide or chloride anions would undoubtedly be hard to overlook in X-ray crystal structure analyses of this type, one could argue that X-ray diffraction does not allow to distinguish ammonia of crystallization from amide anions or ammonium cations, especially if the H atoms of those species cannot be located. In consequence our assignments of charges of the cations and the oxidation states of the U atoms would be wrong. However, “free”, non-coordinating amide anions in the crystal structure can easily be ruled out. As previously reported, NH_2^-

anions are much stronger ligands than NH_3, Cl^-, and Br^- ligands, so that amide ions would coordinate to uranium atoms and could be distinguished from NH_3 ligands by distinctly shorter U−N distances.[27] If the oxidation states of the U_{cen} atoms in the nitride-bridged cations would be lower than stated above, then additional NH_4^+ cations would have to be present. However, ammonium cations in ammoniates are usually surrounded by ammonia molecules in the form of $[NH_4(NH_3)_x]^+$ complexes (x = 1 to 4).[32–36] The $NH_4^+\cdots NH_3$ hydrogen bonds in such $[NH_4(NH_3)_x]^+$ cations are significantly shorter than hydrogen bonds between ammonia molecules of crystallization. To the best of our knowledge, every reported crystal structure containing $[NH_4(NH_3)_x]^+$ cations, shows $NH_4^+\cdots NH_3$ distances in a range from 2.8 to 2.9 Å.[32–36] The absence of such short N···N distances between nitrogen atoms that are not coordinating to U atoms in compounds **1**$Br_8\cdot 26NH_3$, **2**$Br_7\cdot 10.5NH_3$, and **3**$Cl_6\cdot 6NH_3$ indicates the absence of NH_4^+ cations in their crystal structures and our assignments of oxidation states given above appear reasonable. Furthermore, lower oxidation states for uranium than +IV in the complexes are highly unlikely, as the starting materials are the halides of U(V) and uranium(IV) compounds are thermodynamically stable in liquid ammonia under the applied conditions. So, further reduction to U(III) will not occur without an additional reducing agent.[27]

Additional support is given by the isotropic displacement parameters (U_{iso}) of the μ-bridging N atoms which are similar to those of the other N atoms (ammine ligands) in the crystal structures with circa 0.02 in cations $\mathbf{1}^{8+}$ and $\mathbf{2}^{7+}$, and for $\mathbf{3}^{6+}$ with circa 0.013. This indicates that their assignment as N atoms is plausible (see also Supplementary Table 2). If we change the atom assignment for the μ-bridging atoms to O, their isotropic displacement parameters increase to circa 0.03 for **1**$Br_8\cdot 26NH_3$, to circa 0.03 to 0.04 for **2**$Br_7\cdot 10.5NH_3$, and for **3**$Cl_6\cdot 6NH_3$ to 0.02, which does not compare with the other N atoms; it should, however, as O and N have rather similar atomic form factors. This indicates that less electron density than from an O atom occupies the μ-bridging positions. That is, the atom assignment as N instead of O is more plausible. Additionally, the μ-bridging N atoms are tightly bound in between the U_{cen} and U_{ter} atoms, so their displacement ellipsoids should be slightly smaller in comparison to N atoms of ammonia molecules of solvation which are less tightly bound in the crystal structure. This is observed for the μ-bridging atoms being N atoms, but not if they are replaced by O atoms. If we use μ-bridging O atoms and freely refine their site occupancy factors (SOF), they become smaller (see Supplementary Table 2) and deviate much more from unity in comparison. This also indicates that less electron density must occupy this position, so the assignment of the μ-bridging atoms as N instead of O is better.

Raman spectroscopic investigations and ^{15}N labeling studies

The sensitivity of compounds **1**$Br_8 \cdot 26NH_3$, **2**$Br_7 \cdot 10.5NH_3$ and **3**$Cl_6 \cdot 6NH_3$ against air and moisture and especially their rapid decomposition at temperatures above the boiling point of ammonia – if not under pressurized ammonia – prevented many analyses, as at least the transfer of a compound into most analytical instruments must happen at room temperature. However, we were able to obtain Raman spectra in situ by using thin-walled fused silica ampoules as reaction vessels. All spectra of compounds **1**$Br_8 \cdot 26NH_3$ and **3**$Cl_6 \cdot 6NH_3$ (Extended Data Fig. 1) show bands in the region of 888 to 955 cm^{-1}, which can be assigned to the U≡N stretching vibrations of triple bonded uranium nitrides. Organic imido complexes usually show absorption in the 1200 cm^{-1} region, which however is a coupling of the UN and NC resonance.[16] The U=NH stretch in N≡U=N−H is observed at 752 cm^{-1}.[2]

Crystals of **1**$Br_8 \cdot 26NH_3$ grown at −40 °C, as well as their surrounding powder, show a main band at 936 cm^{-1} and two smaller bands at 876 and 955 cm^{-1} (Extended Data Fig. 1). The main band is in accordance with the terminal nitrides [NUF_3] (937 cm^{-1}) and [$UN(N(CH_2CH_2NSi\textit{i}\text{-}Pr_3)_3)$][$Na(12\text{-crown-}4)_2$] (936 cm^{-1}), while a band at 955 cm^{-1} was reported for [$\{U(\mu\text{-}N)(\mu\text{-}Na)(N(CH_2CH_2NSi\textit{i}\text{-}Pr_3)_3)\}_2$], which is close to the 966 cm^{-1} stretch of [N≡U=N−H].[2,18,22] The U≡N stretch of [$UN(N(CH_2CH_2NSi\textit{i}\text{-}Pr_3)_3)$] was observed at 914 cm^{-1}.[14] Four bands at 3145, 3213, 3291 and 3347 cm^{-1} can be assigned to the NH stretch of the ammine ligands.[37] Raman spectra of the mother liquor of **1**$Br_8 \cdot 26NH_3$ show a single band in the U≡N region at 888 cm^{-1} (Extended Data Fig. 1). We assign this to a strong U−N interaction that is weakened in comparison with the one in cation $\mathbf{1}^{8+}$. However, the actual species present in solution remains unknown.

Our simulated Raman spectra for the isolated cations show the symmetric stretching vibration of the U≡N triple bonds of cation $\mathbf{1}^{8+}$ (Extended Data Fig. 2) at 950 cm^{-1} and for free, gas-phase [UN_2] at 1117 cm^{-1}. The deviation compared with the experimental value for the [NUN] molecule inside an argon matrix (1051 cm^{-1}) is due to additional ligands binding to the U_{cen} atom, as also observed for the matrix-isolated [$UN_2(N_2)_x$] complexes (x = 1 to 5).[3,4] Additionally, the matrix effect and the harmonic approximations used in the calculations lead to deviations.[1] Naturally, all [UN_2] molecules coordinated by additional ligands will show bands at lower wavenumbers in comparison to an isolated [N≡U≡N] molecule.

We performed isotope labeling studies and obtained the compounds **2**$Br_7 \cdot 10.5NH_3$ with natural $^{14}N/^{15}N$ isotope ratio, and **2**$Br_7 \cdot 10.5{}^{15}NH_3$ using ^{15}N enriched ammonia. The lattice parameters of both compounds were very similar (see Supplementary Table 1) which shows that we obtained identical compounds except for the ^{15}N enrichment. Thus, a direct comparison of the Raman spectra of the compound with natural $^{14}N/^{15}N$ isotope ratio with the ^{15}N enriched compound became possible (Figure 2). While the band positions of the N−H stretch vibrations are virtually unchanged by the isotope substitution and are observed in the expected range from circa 3158 to 3380 cm^{-1}, the band assigned to the U−N stretch vibration of the central [UN_2] unit, is shifted from 906 to 883 cm^{-1} upon ^{15}N isotope labeling. The isotope shift is circa −23 cm^{-1}, the ratio is 1.026. This value agrees excellently with matrix studies on [$U^{14}N_2$] and [$U^{15}N_2$], where a shift of −22.6 cm^{-1} was reported.[1] In nitrido complexes of iron, also −23 cm^{-1} were observed,[38] while matrix isolation studies on dinitrogen complexes of [UN_2] showed a shift of −31 cm^{-1} with a ratio of 1.031. As shown below, our quantum chemical calculations for cation **2**$^{7+}$ lead, due to the harmonic approximation, to a slightly larger isotope shift of −32 cm^{-1} with a ratio of 1.035. Our Raman measurements confirm also the absence of O atoms, e.g. in the form of [UO_2]$^{2+}$ ions, as then additional U−O bands or no isotope shift would have been observed.

Effects of prolonged storage and room-temperature decomposition

Prolonged storage of compounds **1**$Br_8 \cdot 26NH_3$ and **3**$Cl_6 \cdot 6NH_3$ (see below) in liquid ammonia for several weeks shows them to be only metastable, even at −40 °C. Both decompose to a pale-yellow powder. From the remains of compound **1**$Br_8 \cdot 26NH_3$ the yellow uranium(IV) compound [$U(NH_3)_{10}$]$Br_4 \cdot 9NH_3$ crystallized,[27] and NH_4Br and NH_4Cl, respectively, are present in the decomposition products after evaporation of the solvent ammonia at room temperature. The IR spectra (Extended Data Fig. 3) of these decomposition products show bands assigned to coordinated NH_3 but no signs of any oxidic or [UO_2]$^{2+}$ impurities ($\nu_{as}(UO_2{}^{2+})$: ~911 – 960 cm^{-1}).[39] Bands at 769 and 842 cm^{-1}, which would be in the range assigned to the stretching frequency of $[UO_2]^+$ (~797 cm^{-1}),[40] appear only in the spectrum of the leftovers of **1**$Br_8·26NH_3$. During the Raman measurement at room temperature under pressurized liquid ammonia, crystals of **1**$Br_8·26NH_3$ irreversibly decompose and recrystallize to an unknown compound that shows a single band at 895 cm^{-1} (Supplementary Figure 1), which is still in the range of strong U−N interactions. The Raman spectrum of the surrounding powder reveals a mixture of **1**$Br_8·26NH_3$ and the unknown decomposition product. Compound **3**$Cl_6·6NH_3$ generates a similar spectrum with a major band at 887 cm^{-1}, a small band at 913 cm^{-1} and the U−Cl stretch at 357 cm^{-1}. The calculated value for the symmetric stretch of the U≡N triple bonds in cation $\mathbf{3}^{6+}$ (Extended Data Fig. 2) is 969 cm^{-1}. The deviations are due to the measurement on the solid compounds at room temperature in contrast to the calculations of the cations in the gas phase at 0 K within the harmonic approximation.

Powder X-ray diffraction study of the decomposition product

For an additional indication of the absence of O atoms within the compounds presented here, the room temperature residue of compound **1**$Br_8·26NH_3$ was heated inside a welded steel ampoule under argon to 600 °C and cooled down to room temperature. UNBr[41,42] and UBr_3 were formed as the main products as was shown by powder X-ray diffraction analysis (Extended Data Fig. 4). If O atoms in form of uranyl ions would have been present in **1**$Br_8·26NH_3$, then UO_2 or UO_{2+x} should have been formed during heating in an amount of approximately 30 %, which could not have been overlooked by powder X-ray diffraction. We observe additional reflections of an unknown crystalline phase, which can neither be assigned to any known uranium oxide nor to any known uranyl compound: The strongest additional reflection at 14.1° 2θ (Extended Data Fig. 4) is not matched by any known U-O-phase, while the reflection at circa 28.6° 2θ could belong to the strongest reflection of UO_{2+x}-phases ($x < 1$). However, the next strongest reflections of these phases are not observed in our powder pattern and therefore we deem their presence unlikely.

Quantum chemical calculations

Quantum chemical structure optimizations reproduce the structural motives observed in the solid state (hybrid density functional theory, DFT, see Methods). The calculated U_{cen}≡N distances for cations $\mathbf{1}^{8+}$, $\mathbf{2}^{7+}$, and $\mathbf{3}^{6+}$ (1.83, 1.82, and 1.82 Å, respectively) are only slightly smaller than the observed ones

(Supplementary Table 3) but longer than those calculated for free $[N{\equiv}U{\equiv}N]$ (1.71 Å). This is attributed to the additional ammine, bromido and chlorido ligands, respectively, in cations **1**$^{8+}$, **2**$^{7+}$, and **3**$^{6+}$ as can be shown by comparison with a hypothetical $[UN_2(NH_3)_5]$ complex, which is analogous to the known $[UO_2(NH_3)_5]^{2+}$ cation.[27] Here, the U≡N distance increases to 1.77 Å, which is much closer to the distances observed in cations **1**$^{8+}$, **2**$^{7+}$, and **3**$^{6+}$. This is compliant with the elongated U≡N distance in matrix isolated $[UN_2(N_2)_5]$.[4] We investigated the bonding in the cations by using Intrinsic Bond Orbitals (IBOs, see Methods) (Figure 3 and Extended Data Fig. 5).[43] The IBOs of the $[UN_2]$ moiety of cation **1**$^{8+}$ (Figure 3) prove to be very similar to free $[UN_2]$ and the U_{cen} contribution is only slightly lessened due to the coordination of the five ammine ligands. With two σ- and four π-bonds, we propose the formulation of the $[UN_2]$ species as $[N{\equiv}U{\equiv}N]$. The IBO analysis of free $[UN_2]$ is in line with the canonical molecular orbital analysis presented for $[UN_2]$ previously.[2,44,45]

While the Lewis structure is consistent with that of the uranyl ion, $[O{\equiv}U{\equiv}O]^{2+}$, the differences in electronegativity of N and O influence the extent of covalence of the triple bonding. The bonding analysis (Supplementary Table 4) shows the bonds in free $[UN_2]$ to be the most covalent. The ionic character of the $U{\equiv}X$ triple bonds (X = N, O) increases from $[UN_2(NH_3)_5]$ over cations **1**$^{8+}$, **2**$^{7+}$, and **3**$^{6+}$, to free $[UO_2^{2+}]$ and $[UO_2(NH_3)_5]^{2+}$, as the contribution of the U atom to the σ- and π-orbitals decreases in this order. The Intrinsic Atomic Orbital (IAO) partial charges of free $[UN_2]$ are in agreement with the CASSCF Mulliken partial charges reported previously.[2] The U atoms of cations **1**$^{8+}$, **2**$^{7+}$, and **3**$^{6+}$ naturally carry a higher partial charge compared with neutral $[UN_2(NH_3)_5]$. However, despite their oxidation state of +VI, the U_{cen} atoms only carry partial charges of +0.78, +0.72 and +0.70, respectively, as a result of the covalent character of the U≡N triple bonds. The IBOs (Extended Data Fig. 5) indicate a U_{ter}−(μ-N) interaction which is similar to the $U{-}NH_3$ contacts. This is represented by the dative single bonds in the Lewis pictures given in Figure 1).

Conclusion

The $[UN_2]$ molecule is the isoelectronic analogue of the uranyl cation $[UO_2]^{2+}$ and was observed for the first time outside matrix conditions. From reactions of UCl_5 and UBr_5 in liquid anhydrous ammonia we obtained the three compounds **1**$Br_8{\cdot}26NH_3$, **2**$Br_7{\cdot}10.5NH_3$, and **3**$Cl_6{\cdot}6NH_3$. The linear $[UN_2]$ molecules are contained in the center of the trinuclear complex cations $\mathbf{1}^{8+}$, $\mathbf{2}^{7+}$, and $\mathbf{3}^{6+}$ and their U atoms are additionally coordinated by five ligands $[\mathrm{UN_2(NH_3)}_{5-x}L_x]^{x-}$ with $x = 0$ for $\mathbf{1}^{8+}$, $x = 1$ and L = Br for $\mathbf{2}^{7+}$, and $x = 2$ and L = Cl for $\mathbf{3}^{6+}$. Additionally, the N atoms of the [N≡U≡N] moiety are coordinated by $[\mathrm{U(NH_3)_8}]^{4+}$ units to form the trinuclear cations $[\mathrm{(H_3N)_8U{-}\{UN_2(NH_3)}_{5-x}L_x\}\mathrm{{-}U(NH_3)_8}]^{(8-x)+}$. Structural, crystal-chemical, and crystallographic considerations as well as powder X-ray diffraction analysis on annealed samples suggest the absence of O-containing species, such as $[\mathrm{UO_2}]^{2+}$ or $[\mathrm{UO_2}]^{+}$, in the compounds. The absence of such O-species was shown with ^{15}N-isotope labeling as besides the isotope-shifted U≡N band no U≡O bands are observed in the Raman spectrum. Quantum chemical calculations showed that the chemical bonds in the [$\mathrm{UN_2}$] moieties are best described with U≡N triple bonds.

References

1. Hunt, R. D., Yustein, J. T. & Andrews, L. Matrix infrared spectra of NUN formed by the insertion of uranium atoms into molecular nitrogen. *J. Chem. Phys.* **98**, 6070–6074 (1993).
2. Wang, X., Andrews, L., Vlaisavljevich, B. & Gagliardi, L. Combined Triple and Double Bonds to Uranium: The N≡U═N−H Uranimine Nitride Molecule Prepared in Solid Argon. *Inorg. Chem.* **50**, 3826–3831 (2011).
3. Andrews, L. *et al.* Infrared Spectra and Electronic Structure Calculations for NN Complexes with U, UN, and NUN in Solid Argon, Neon, and Nitrogen. *J. Phys. Chem. A* **118**, 5289–5303 (2014).
4. Andrews, L., Wang, X., Gong, Y., Vlaisavljevich, B. & Gagliardi, L. Infrared Spectra and Electronic Structure Calculations for the $\mathrm{NUN(NN)_{1–5}}$ and $\mathrm{NU(NN)_{1–6}}$ Complexes in Solid Argon. *Inorg. Chem.* **52**, 9989–9993 (2013).
5. Falcone, M., Chatelain, L., Scopelliti, R., Živković, I. & Mazzanti, M. Nitrogen reduction and functionalization by a multimetallic uranium nitride complex. *Nature* **547**, 332–335 (2017).

6. Cleaves, P. A. *et al.* Terminal Uranium(V/VI) Nitride Activation of Carbon Dioxide and Carbon Disulfide: Factors Governing Diverse and Well-Defined Cleavage and Redox Reactions. *Chem. Eur. J.* **23**, 2950–2959 (2017).
7. Falcone, M., Poon, L. N., Fadaei, T. F. & Mazzanti, M. Reversible Dihydrogen Activation and Hydride Transfer by a Uranium Nitride Complex. *Angew. Chem., Int. Ed.* **57**, 3697–3700 (2018).
8. Fox, A. R., Bart, S. C., Meyer, K. & Cummins, C. C. Towards uranium catalysts. *Nature* **455**, 341–349 (2008).
9. Fox, A. R., Arnold, P. L. & Cummins, C. C. Uranium−Nitrogen Multiple Bonding: Isostructural Anionic, Neutral, and Cationic Uranium Nitride Complexes Featuring a Linear U═N═U Core. *J. Am. Chem. Soc.* **132**, 3250–3251 (2010).
10. Rogozkin, B. D., Stepennova, N. M., Bergman, G. A. & Proshkin, A. A. Thermochemical Stability, Radiation Testing, Fabrication, and Reprocessing of Mononitride Fuel. *At. Energ.* **95**, 835–844 (2003).
11. Matthews, R. B., Chidester, K. M., Hoth, C. W., Mason, R. E. & Petty, R. L. Fabrication and testing of uranium nitride fuel for space power reactors. *J. Nucl. Mater.* **151**, 345–345 (1988).
12. Diaconescu, P. Actinide chemistry: A tale of two nitrides. *Nat. Chem.* **2**, 705–706 (2010).
13. *Technology Roadmap Update for Generation IV Nuclear Energy Systems*. (2014).
14. King, D. M. *et al.* Isolation and characterization of a uranium(VI)–nitride triple bond. *Nat. Chem.* **5**, 482–488 (2013).
15. Gardner, B. M. *et al.* Triamidoamine uranium(IV)–arsenic complexes containing one-, two- and threefold U–As bonding interactions. *Nat. Chem.* **7**, 582–590 (2015).
16. Hayton, T. W. *et al.* Synthesis of Imido Analogs of the Uranyl Ion. *Science* **310**, 1941–1943 (2005).
17. King, D. M. & Liddle, S. T. Progress in molecular uranium-nitride chemistry. *Coord. Chem. Rev.* **266/267**, 2–15 (2014).

18. King, D. M. *et al.* Synthesis and Structure of a Terminal Uranium Nitride Complex. *Science* **337**, 717–720 (2012).

19. Camp, C., Pécaut, J. & Mazzanti, M. Tuning Uranium–Nitrogen Multiple Bond Formation with Ancillary Siloxide Ligands. *J. Am. Chem. Soc.* **135**, 12101–12111 (2013).

20. Evans, W. J., Kozimor, S. A. & Ziller, J. W. Molecular Octa-Uranium Rings with Alternating Nitride and Azide Bridges. *Science* **309**, 1835–1838 (2005).

21. Kushto, G. P., Souter, P. F. & Andrews, L. An infrared spectroscopic and quasirelativistic theoretical study of the coordination and activation of dinitrogen by thorium and uranium atoms. *J. Chem. Phys.* **108**, 7121–7130 (1998).

22. Andrews, L., Wang, X., Lindh, R., Roos, B. O. & Marsden, C. J. Simple $N\equiv UF_3$ and $P\equiv UF_3$ Molecules with Triple Bonds to Uranium. *Angew. Chem., Int. Ed.* **47**, 5366–5370 (2008).

23. Fox, A. R. & Cummins, C. C. Uranium−Nitrogen Multiple Bonding: The Case of a Four-Coordinate Uranium(VI) Nitridoborate Complex. *J. Am. Chem. Soc.* **131**, 5716–5717 (2009).

24. Evans, W. J., Miller, K. A., Ziller, J. W. & Greaves, J. Analysis of Uranium Azide and Nitride Complexes by Atmospheric Pressure Chemical Ionization Mass Spectrometry. *Inorg. Chem.* **46**, 8008–8018 (2007).

25. Anderson, N. H. *et al.* Elucidating bonding preferences in tetrakis(imido)uranate(VI) dianions. *Nat. Chem.* **9**, 850–855 (2017).

26. Schmidt, A.-C., Heinemann, F. W., Maron, L. & Meyer, K. A Series of Uranium(IV, V, VI) Tritylimido Complexes, Their Molecular and Electronic Structures and Reactivity with CO_2. *Inorg. Chem.* **53**, 13142–13153 (2014).

27. Rudel, S. S. *et al.* Recent advances in the chemistry of uranium halides in anhydrous ammonia. *Z. Kristallogr. - Cryst. Mater.* **233**, 817–844 (2018).

28. Jean-Claude Berthet, Gerald Siddredi, Pierre Thuery & Michel Ephritikhine. Synthesis and crystal structure of pentavalent uranyl complexes. The remarkable stability of UO_2X(X = I, SO_3CF_3) in non-aqueous solutions. *Dalton Trans.* 3478–3494 (2009).

29. Berthet, J.-C., Nierlich, M., Miquel, Y., Madic, C. & Ephritikhine, M. Selective complexation of uranium(III) over lanthanide(III) triflates by 2,2′:6′,2″-terpyridine. X-Ray crystal structures of $[M(OTf)_3(terpy)_2]$ and $[M(OTf)_2(terpy)_2(py)][OTf]$ (M = Nd, Ce, U) and of polynuclear μ-oxo uranium(IV) complexes resulting from hydrolysis. *Dalton Trans.* 369–379 (2005).

30. Fortier, S., Brown, J. L., Kaltsoyannis, N., Wu, G. & Hayton, T. W. Synthesis, Molecular and Electronic Structure of $U^{V}(O)[N(SiMe_3)_2]_3$. *Inorg. Chem.* **51**, 1625–1633 (2012).

31. Gardner, B. M. *et al.* Homologation and functionalization of carbon monoxide by a recyclable uranium complex. *Proc. Natl. Acad. Sci. U. S. A.* **109**, 9265–9270 (2012).

32. Olovsson, I. The crystal structures of the triammines of the ammonium halides. *Acta Chem. Scand.* **14**, 1453–1465 (1960).

33. Olovsson, I. The Crystal Structure of Tetrammineammonium Iodide. *Acta Chem. Scand.* **14**, 1466–1474 (1960).

34. Roßmeier, T. Supramolekulare Chemie mit Ammoniak – Strukturchemie neuer Ammoniak-Proton-Komplexe. (Regensburg, 2005).

35. Roßmeier, T., Reil, M. & Korber, N. First Characterization of the Ammine−Ammonium Complex $[\{NH_4(NH_3)_4\}_2(\mu\text{-}NH_3)_2]^{2+}$ in the Crystal Structure of $[NH_4(NH_3)_4][B(C_6H_5)_4]\cdot NH_3$ and the $[NH_4(NH_3)_4]^+$ Complex in $[NH_4(NH_3)_4][Ca(NH_3)_7]As_3S_6\cdot 2NH_3$ and $[NH_4(NH_3)_4][Ba(NH_3)_8]As_3S_6\cdot NH_3$. *Inorg. Chem.* **43**, 2206–2212 (2004).

36. Roßmeier, T. & Korber, N. First Characterization of an Extended Ammonium-Ammonia Complex $[NH_4(NH_3)_4^+(\mu\text{-}NH_3)_2]$ in the Crystal Structure of $[NH_4(NH_3)_4][Co(C_2B_9H_{11})_2]\cdot 2NH_3$. *Z. Anorg. Allg. Chem.* **630**, 2665–2668 (2004).

37. Schmidt, K. H. & Müller, A. Vibrational Spectra and Force Constants of Pure Ammine Complexes. *Coord. Chem. Rev.* **19**, 41–97 (1976).

38. Wagner, W. D. & Nakamoto, K. Resonance Raman spectra of nitridoiron(V) porphyrin intermediates produced by laser photolysis. *J. Am. Chem. Soc.* **111**, 1590–1598 (1989).

39. Bullock, J. I. Raman and infrared spectroscopic studies of the uranyl ion: the symmetric stretching frequency, force constants, and bond lengths. *J. Chem. Soc. A* 781 (1969).

40. Nocton, G. *et al.* Synthesis, Structure, and Bonding of Stable Complexes of Pentavalent Uranyl. *J. Am. Chem. Soc.* **132**, 495–508 (2010).

41. Juza, R. & Meyer, W. Über Uran-Nitrid-Chlorid, -Bromid und -Jodid. *Z. Anorg. Allg. Chem.* **366**, 43–50 (1969).

42. Murasik, A., Furrer, A. & Szczepaniak, W. Crystal-field levels in UBr3 determined by neutron spectroscopy. *Solid State Communications* **33**, 1217–1219 (1980).

43. Knizia, G. Intrinsic Atomic Orbitals: An Unbiased Bridge between Quantum Theory and Chemical Concepts. *J. Chem. Theory Comput.* **9**, 4834–4843 (2013).

44. Kaltsoyannis, N. Computational Study of Analogues of the Uranyl Ion Containing the −NUN− Unit: Density Functional Theory Calculations on UO_2^{2+}, UON^+, UN_2, $UO(NPH_3)^{3+}$, $U(NPH_3)_2^{4+}$, $[UCl_4\{NPR_3\}_2]$ (R = H, Me), and $[UOCl_4\{NP(C_6H_5)_3\}]^-$. *Inorg. Chem.* **39**, 6009–6017 (2000).

45. Wei, F., Wu, G., Schwarz, W. H. E. & Li, J. Geometries, electronic structures, and excited states of UN_2, NUO^+, and UO_2^{2+}: a combined CCSD(T), RAS/CASPT2 and TDDFT study. *Theor. Chem. Acc.* **129**, 467–481 (2011).

Acknowledgement

S.S. Rudel and F. Kraus thank the Deutsche Forschungsgemeinschaft for generous funding. A. J. Karttunen thanks CSC, the Finnish IT Center for Science, for computational resources. We thank Bernd Roling for using his Raman spectrometer. We thank Ulrich Müller to bring [UN_2] to our attention many years ago.

Author Contributions

S.S.R. conceived and designed experiments, interpreted crystal structures, powder patterns and spectra on $\mathbf{1}^{8+}$ and $\mathbf{3}^{6+}$. S.S.R. and M.M. performed experiments and analytics on $\mathbf{1}^{8+}$ and $\mathbf{3}^{6+}$. M.M. contributed to the manuscript. H.L.D. conceived, designed and performed experiments on $\mathbf{2}^{7+}$. H.L.D. and M.M.

interpreted the single-crystal structure of **2**$^{7+}$. H.L.D. and M.M. contributed equally to the manuscript. A.J.K. conceived and designed the quantum chemical calculations, interpreted results, wrote the theoretical parts of the manuscript. F.K. designed and guided research, interpreted the single-crystal structure determinations, powder patterns, spectra. S.S.R. and F.K. wrote the manuscript. All authors discussed the results and commented on the manuscript.

Competing Interests Statement

The authors declare no competing interests.

Figure Legends

Figure 1. Representative Lewis structures and structures of the cations **1**$^{8+}$, **2**$^{7+}$, and **3**$^{6+}$ in their crystal structures, showing the central [N≡U≡N] units. L denotes NH_3 ligands. U atoms are green, N atoms blue, Br atoms brown, and Cl atoms dark green. Anisotropic displacement ellipsoids are shown at 70 % probability level at 100 K. a) Cation **1**$^{8+}$. b) Cations **2**$^{7+}$; both crystallographically independent molecules are shown. The U−Br bonds are 2.9790(11) and 2.9689(11) Å in length. c) Cation **3**$^{6+}$. The U−Cl bonds are 2.8071(14) and 2.8365(14) Å in length.

Figure 2. Raman spectra of the compound **2**$Br_7 \cdot 10.5NH_3$ with natural $^{14}N/^{15}N$ isotope ratio and the isotope labelled compound with $^{15}NH_3$. a) Raman spectrum of the compound with NH_3 in natural isotope ratio. b) Raman spectrum of the compound with ^{15}N enriched ammonia. The bands in the range from circa 3158 to 3380 cm^{-1} are assigned to symmetric and asymmetric N−H stretch vibrations of NH_3 molecules, while the band at 906 (in a) and 883 cm^{-1} (in b) is assigned to the U−N and U−^{15}N vibration within the central [UN_2] and [$U^{15}N_2$] moieties. The isotope shift is circa −23 cm^{-1}, ratio 1.026.

Figure 3. Intrinsic Bond Orbitals (IBOs) corresponding to the U≡N triple bonds in the [UN_2] molecule and cation **1**$^{8+}$. The red and green orbitals are the IBOs, while cyan, blue, and white denote U, N, and H atoms, respectively. a) shows the σ-bonds in [UN_2] and **1**$^{8+}$, b) shows the first set of π-bonds for [UN_2] and **1**$^{8+}$, and c) shows the second set of π-bonds. The listed percentages show the contribution of each atom in the IBO. In a purely covalent two-atomic bond, each atom would contribute 50%. The isovalue for IBO isosurface plots is 0.08 a.u.

Methods

All work was carried out under the exclusion of moisture and air in an atmosphere of dried and purified argon (Praxair 5.0, passed through titanium sponge at 800 °C) using vacuum glass lines or a glove box (MBraun). All glass vessels were flame dried under vacuum before use. Liquid ammonia (Air Liquide, 99.98%) was dried and stored over sodium (VWR) in a special vacuum glass line. BCl_3 (Merck, >99%) was distilled *in vacuo* and portioned into flame sealed glass ampoules. U turnings were washed with nitric acid, deionized and degassed water, then acetone, and dried in vacuum before use. Br_2 was stirred with P_4O_{10}, sublimed twice and stored over fresh P_4O_{10}. UF_5 was synthesized by the photoreduction of UF_6 with CO.[46] UCl_5 was synthesized by metathesis of UF_5 and BCl_3 in FEP-vessels which were dried in *in vacuo* at 100 °C.[47] UBr_5 was prepared from the elements.[27,48] The purity of both compounds was checked with powder X-ray diffraction, IR and Raman spectroscopy (Supplementary Figures 1-4).

$[U_3(\mu\text{-}N)_2(NH_3)_{21}]Br_8\cdot 26NH_3$ ($\mathbf{1}Br_8\cdot 26NH_3$), Henicosaammine-1κ^8*N*,2κ^8*N*,3κ^5*N*-di-μ-nitrido-1:3κ^2*N*;2:3κ^2*N*-diuranium(4+)uranium(6+) bromide – ammonia(1/26)

UBr_5 (220 mg, 0.35 mmol) was treated with liquid ammonia (~5 mL) inside a reaction tube at –78 °C. After two weeks of storage at –40 °C, green flat rod-shaped crystals of compound $\mathbf{1}Br_8\cdot 26NH_3$ admixed with NH_4Br and an unknown powder were obtained.

$[(NH_3)_8U(\mu\text{-}N)Br(NH_3)_4U(\mu\text{-}N)U(NH_3)_8]_2Br_{14}\cdot 21NH_3$, ($\mathbf{2}Br_7\cdot 10.5NH_3$), Eicosaammine-1κ^8*N*,2κ^8*N*,3κ^4*N*-bromido-3κ^1*Br*-di-μ-nitrido-1:3κ^2*N*;2:3κ^2*N*-diuranium(4+)uranium(6+) bromide – ammonia(1/21)

UBr_5 (15 mg, 0.024 mmol) was treated with liquid ammonia or ^{15}N-ammonia (~0.25 mL) inside a flame sealed silica ampoule (bomb tube, 4 mm outer diameter) for ten days at −35 °C. The bomb tube was sealed in vacuo at −196 °C. After three to four weeks of storage at room temperature green plate-shaped crystals of compound $\mathbf{2}Br_7\cdot 10.5NH_3$ admixed with NH_4Br were obtained.

$[U_3Cl_2(\mu\text{-}N)_2(NH_3)_{19}]Cl_6\cdot 6NH_3$, ($\mathbf{3}Cl_6\cdot 6NH_3$), Nonadecaammine-1κ^8*N*,2κ^8*N*,3κ^3*N*-dichlorido-3κ^2*Cl*-di-μ-nitrido-1:3κ^2*N*;2:3κ^2*N*-diuranium(4+)uranium(6+) chloride – ammonia(1/6)

UCl_5 (33 mg, 0.08 mmol) was treated with liquid ammonia (~5 mL) in a flame sealed glass ampoule at –78 °C. The tube was sealed in vacuo at −196 °C. After six weeks of storage at room temperature green rod-shaped crystals of compound $\mathbf{3}Cl_6\cdot 6NH_3$ and NH_4Cl powder were obtained.

Powder X-ray diffraction: Powder X-Ray diffraction patterns were recorded inside flame sealed borosilicate glass capillaries by using a STOE Stadi MP powder diffractometer with germanium monochromated $Cu_{K\alpha 1}$ radiation and a Mythen1K detector. Phase analysis was carried out with the WinXPOW software package.[49]

Single-crystal X-ray analyses: Single crystals were extracted from liquid ammonia at –78 °C, selected under exclusion of air in cooled perfluorinated polyether (Galden LS 230, Solvay Solexis) and mounted using the MiTeGen MicroLoop system. Data were collected at −173 K using a Stoe IPDS2/2T diffractometer with Mo-K_α (λ = 0.71073 Å) and processed with the Stoe X-Area software.[50] The diffraction data were scaled with the Laue Analyzer in X-Area and corrected for absorption with the X-Red and X-Shape software.[51–53] The structures were solved by using Direct Methods (SHELXS-97 (**1**$Br_8{\cdot}26NH_3$) and SHELXT-14/5 (**2**$Br_7{\cdot}10.5NH_3$, **3**$Cl_6{\cdot}6NH_3$))[54,55] and refined against F^2 (SHELXL-2016/6)[56] using the ShelXle software package.[57] The crystal structure of **1**$Br_8{\cdot}26NH_3$ contains a large amount of ammonia of crystallization. We refined the nitrogen atoms of the ammonia molecules of solvation N47 to N49 as split positions and N48 and N49 with the SUMP command, as these atoms are heavily disordered inside channels along the *c* axis at *z* = 1/2. For the ammonia molecules, located on split positions, as well as those with the nitrogen atoms N38, N42, N43, N46, the H atoms could not be located from the electron density map.

IR Spectroscopy: IR Spectra were recorded by using the PLATINUM ATR module on a Bruker Alpha FT-IR spectrometer with a spectral resolution of 4 cm^{-1} inside a glovebox. The data were treated with the OPUS software package and Origin 2017.[58]

Raman Spectroscopy: Raman spectra were recorded for **1**$Br_8{\cdot}26NH_3$ and **3**$Cl_6{\cdot}6NH_3$ with a Renishaw Raman microscope, using a frequency-doubled Nd:YAG Laser (532 nm wavelength). For **2**$Br_7{\cdot}10.5NH_3$, the Raman spectra were measured at room temperature with a Monovista CRS+ confocal Raman microscope (Spectroscopy & Imaging GmbH) using a 532 nm solid-state laser. We reacted UBr_5 and UCl_5, respectively, inside a flame-sealed fused silica tube with 0.5 mm wall thickness and 4 mm diameter. One sample of UBr_5 in ammonia was kept at −36 °C until the measurement. The other samples were stored at room temperature for three days. Crystals, precipitated powder as well as the solutions, were subjected to Raman spectroscopy inside these tubes under the pressure of liquid ammonia at room temperature.

Computational details: Quantum chemical calculations were carried out using the TURBOMOLE program package.[59,60] We used the PBE0 hybrid density functional method and a triple-zeta-valence quality basis set with polarization functions (def-TZVP).[61–64] Scalar relativistic effects were taken into account by applying a 60-electron relativistic effective core potential for U.[65] Multipole-accelerated resolution-of-the-identity technique was used to speed up the calculations.[66–68] Cations **1**–**3** were fully optimized without any symmetry constraints (C_1 point group), cartesian coordinates are available in Source Data 2. $[UN_2(NH_3)_5]$ and $[UO_2(NH_3)_5]^{2+}$ were optimized in the C_{5h} point group, while for $[UN_2]$ and $[UO_2]^{2+}$, the D_{6h} point group was applied. Because the molecular calculations of the cations **1**–**3** lack the counteranions present in the solids, we applied the COSMO continuum solvation model to counter the rather high positive charge of the cations.[69] Harmonic frequency calculations were carried out on the optimized structures. For $\mathbf{1}^{8+}$, two imaginary frequencies corresponding to rotational motion of two ammonia ligands persisted even after several re-optimizations carried out by following the imaginary modes (350*i* and 224*i* cm^{-1}). The imaginary modes probably arise because the highly charged (8+) cation has been cut out from the crystal field and embedded in a COSMO solvent field. Cations $\mathbf{2}^{7+}$ and $\mathbf{3}^{6+}$ with slightly lower charge do not show any imaginary modes. Molecular $[UN_2]$, $[UO_2]^{2+}$, $[UN_2(NH_3)_5]$ and $[UO_2(NH_3)_5]^{2+}$ were also confirmed to be true local minima. In the Raman spectrum calculations (λ = 532 nm; T = 298.15 K, unpolarized radiation, scattering angle of 90°),[70] the COSMO solvent model was not used in the calculation of the ground state or the dynamic polarizability derivatives. The Raman intensities are given relative to the most intensive peak. The final Raman spectra were convoluted using Lorenzian peak profiles with FWHM of 20 cm^{-1}. Intrinsic Atomic Orbitals (IAOs) and Bond Orbitals (IBOs) were used in the bonding analysis.[43,71] For the IAO and IBO analysis of uranium, we used free-atom reference orbitals that are described in Source Data 1.

Additional details for the IBO reference orbitals

Like molecular orbitals, IBOs are not physical observables, but they can be considered as a physically well-defined form of localized molecular orbitals (MOs) designed for chemical interpretation.[43,71] While delocalized canonical molecular orbitals are often difficult to connect to textbook-level chemical concepts, IBOs are a powerful technique to represent wavefunctions in an exact and a simple way.

The listed percentages (Figure 3, Supplementary Table 4, Extended Data Fig. 5) show the contribution of each atom in the IBO (if the percentages do not add up exactly to 100%, some other atoms are giving minor contributions smaller than 1%). The interpretation of the IBOs is rather simple: In a purely covalent two-atomic bond, each atom would contribute 50%. The further the contributions differ from 50%, the more ionic the bond is. There can also be some minor contributions from other atoms.

Generation of IBOs requires a set of reference orbitals that have been obtained for an isolated atom and Knizia proposed to derive the reference orbitals from the triple-zeta-valence cc-pVTZ basis set.[43,71] The TURBOMOLE basis set library includes IBO reference orbitals based on cc-pVTZ or cc-pVTZ-PP basis sets for most elements, but there are no reference orbitals for uranium. We derived a set of reference orbitals for the uranium $5f^3 6d^1 7s^2$ ground state (Restricted-Open HF with Roothaan parameters a = 21/26, b = 21/26). The reference orbitals (TURBOMOLE format, Supplementary Data 4) were obtained for the def-TZVP basis set (without polarization functions).[63,64] We also checked that the IBO results were similar with reference orbitals obtained for the uranium cc-pVTZ-PP basis set.

References for methods section

27. Rudel, S. S. *et al.* Recent advances in the chemistry of uranium halides in anhydrous ammonia. *Z. Kristallogr. - Cryst. Mater.* **233**, 817–844 (2018).
46. Scheibe, B., Rudel, S. S., Buchner, M. R., Karttunen, A. J. & Kraus, F. A 1D Coordination Polymer of UF_5 with HCN as a Ligand. *Chem. - Eur. J.* **23**, 291–295 (2017).
47. Brown, D., Berry, J. A. & Holloway, J. H. Halogen exchange reactions involving uranium-(V) and -(VI) halides. *J. Chem. Soc., Dalton Trans.* 1385–1388 (1982).
48. Deubner, H. L. *et al.* A Revised Structure Model for the UCl_6 Structure Type, Novel Modifications of UCl_6 and UBr_5, and a Comment on the Modifications of Protactinium Pentabromides. *Chem. Eur. J.* **25**, 6402–6411 (2019).
49. *STOE WinXPOW*. (STOE & Cie GmbH, 2015); https://www.stoe.com/
50. *X-Area*. (STOE & Cie GmbH, 2018); https://www.stoe.com/
51. *X-RED32*. (STOE & Cie GmbH, 2012); https://www.stoe.com/

52. *X-SHAPE*. (STOE & Cie GmbH, 2013); https://www.stoe.com/

53. *LANA - Laue Analyzer*. (STOE & Cie GmbH, 2019); https://www.stoe.com/

54. Sheldrick, G. M. *SHELXS-97*. (1997); http://shelx.uni-ac.gwdg.de/SHELX/index.php

55. Sheldrick, G. M. SHELXT – Integrated space-group and crystal-structure determination. *Acta Crystallogr., Sect. A: Found. Adv.* **71**, 3–8 (2015).

56. Sheldrick, G. M. *SHELXL-2016/6*. (2016); http://shelx.uni-ac.gwdg.de/SHELX/index.php

57. Hübschle, C. B., Sheldrick, G. M. & Dittrich, B. ShelXle: a Qt graphical user interface for SHELXL. *J. Appl. Crystallogr.* **44**, 1281–1284 (2011).

58. *OPUS*. (Bruker Optik GmbH, 2009); https://www.bruker.com/

59. Ahlrichs, R., Bär, M., Häser, M., Horn, H. & Kölmel, C. Electronic structure calculations on workstation computers: The program system turbomole. *Chem. Phys. Lett.* **162**, 165–169 (1989).

60. Turbomole versions 7.2 and 7.3. University of Karlsruhe and Forschungszentrum Karlsruhe GmbH. *TURBOMOLE*. (TURBOMOLE GmbH, 2017); http://www.turbomole.com

61. Perdew, J. P., Burke, K. & Ernzerhof, M. Generalized Gradient Approximation Made Simple. *Phys. Rev. Lett.* **77**, 3865–3868 (1996).

62. Adamo, C. & Barone, V. Toward reliable density functional methods without adjustable parameters: The PBE0 model. *J. Chem. Phys.* **110**, 6158–6170 (1999).

63. Schäfer, A., Huber, C. & Ahlrichs, R. Fully optimized contracted Gaussian basis sets of triple zeta valence quality for atoms Li to Kr. *J. Chem. Phys.* **100**, 5829–5835 (1994).

64. Cao, X. & Dolg, M. Segmented contraction scheme for small-core actinide pseudopotential basis sets. *J. Mol. Struct.: THEOCHEM* **673**, 203–209 (2004).

65. W. Küchle, M. Dolg, H. Stoll & H. Preuss. Energy-adjusted pseudopotentials for the actinides. Parameter sets and test calculations for thorium and thorium monoxide. *J. Chem. Phys.* **100**, 7535–7542 (1994).

66. Eichkorn, K., Treutler, O., Öhm, H., Häser, M. & Ahlrichs, R. Auxiliary basis sets to approximate Coulomb potentials. *Chem. Phys. Lett.* **240**, 283–290 (1995).

67. Weigend, F. Accurate Coulomb-fitting basis sets for H to Rn. *Phys. Chem. Chem. Phys.* **8**, 1057–1065 (2006).

68. Sierka, M., Hogekamp, A. & Ahlrichs, R. Fast evaluation of the Coulomb potential for electron densities using multipole accelerated resolution of identity approximation. *J. Chem. Phys.* **118**, 9136–9148 (2003).

69. Klamt, A. & Schürmann, G. COSMO: a new approach to dielectric screening in solvents with explicit expressions for the screening energy and its gradient. *J. Chem. Soc., Perkin Trans.* **2** 799–805 (1993).

70. Rappoport, D. & Furche, F. Lagrangian approach to molecular vibrational Raman intensities using time-dependent hybrid density functional theory. *J. Chem. Phys.* **126**, 201104 (2007).

71. Knizia, G. & Klein, J. E. M. N. Electron Flow in Reaction Mechanisms—Revealed from First Principles. *Angew. Chem. Int. Ed.* **54**, 5518–5522 (2015).

Data availability statement

Crystal Structure Data were deposited with The Cambridge Crystallographic Data Centre (depository numbers 1868199 for **3**$Cl_6 \cdot 6NH_3$, 1868200 for **1**$Br_8 \cdot 26NH_3$, 1984956 for **2**$Br_7 \cdot 10.5NH_3$) and within the Supplementary Information. Powder X-ray patterns, Raman and IR spectra and details of the quantum chemical calculations are in the Supplementary Information.

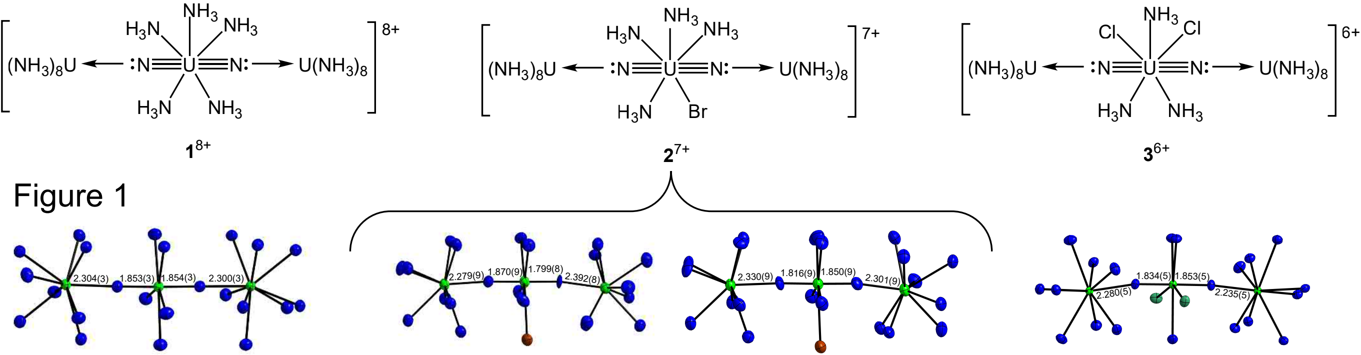
(NH3)8U ← :N≡U≡N: → U(NH3)8
H3N
NH3
NH3
H3N
NH3
8+
1^8+
(NH3)8U ← :N≡U≡N: → U(NH3)8
H3N
NH3
NH3
H3N
Br
7+
2^7+
(NH3)8U ← :N≡U≡N: → U(NH3)8
Cl
NH3
Cl
H3N
NH3
6+
3^6+
2.304(3)
1.853(3)
1.854(3)
2.300(3)
2.279(9)
1.870(9)
1.799(8)
2.392(8)
2.330(9)
1.816(9)
1.850(9)
2.301(9)
1.834(5)
1.853(5)
2.280(5)
2.235(5)

Figure 1

Figure 2

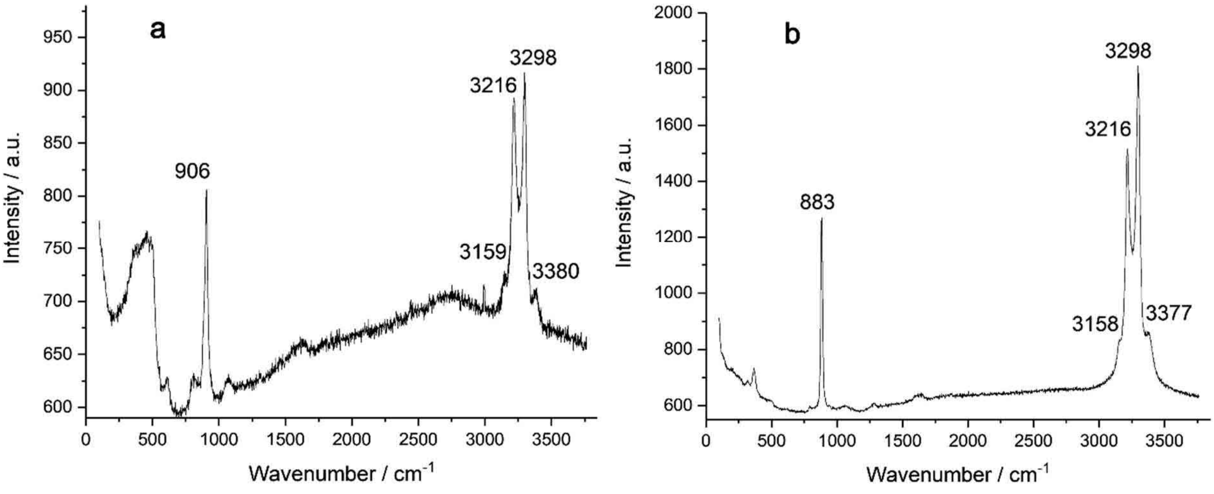
a
Intensity / a.u.
950
900
850
800
750
700
650
600
906
3159
3216
3298
3380
0
500
1000
1500
2000
2500
3000
3500
Wavenumber / cm^{-1}
b
Intensity / a.u.
2000
1800
1600
1400
1200
1000
800
600
883
3158
3216
3298
3377
0
500
1000
1500
2000
2500
3000
3500
Wavenumber / cm^{-1}

Figure 3

a Two σ-bonding IBOs

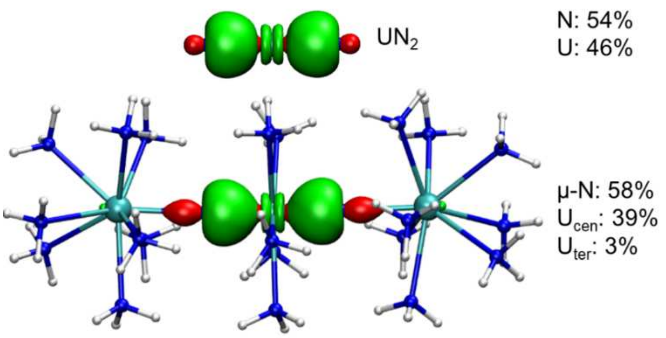

b Two π-bonding IBOs (first set)

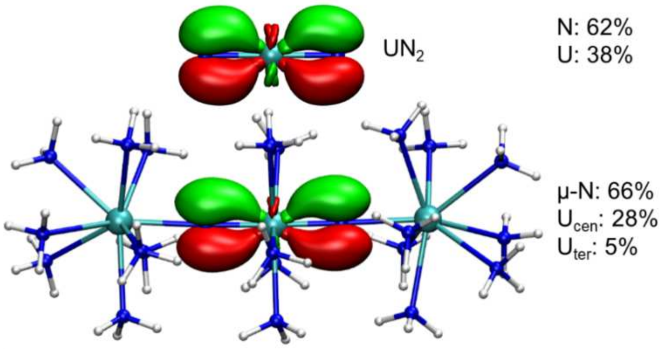

c Two π-bonding IBOs (second set)